



HAL
open science

Improved one-shot total energies from the linearized GW density matrix

Fabien Bruneval, Mauricio Rodriguez, Patrick Rinke, Marc Dvorak

► **To cite this version:**

Fabien Bruneval, Mauricio Rodriguez, Patrick Rinke, Marc Dvorak. Improved one-shot total energies from the linearized GW density matrix. *Journal of Chemical Theory and Computation*, 2021, 17, pp.2126. 10.1021/acs.jctc.0c01264 . cea-03325695

HAL Id: cea-03325695

<https://cea.hal.science/cea-03325695>

Submitted on 25 Aug 2021

HAL is a multi-disciplinary open access archive for the deposit and dissemination of scientific research documents, whether they are published or not. The documents may come from teaching and research institutions in France or abroad, or from public or private research centers.

L'archive ouverte pluridisciplinaire **HAL**, est destinée au dépôt et à la diffusion de documents scientifiques de niveau recherche, publiés ou non, émanant des établissements d'enseignement et de recherche français ou étrangers, des laboratoires publics ou privés.

Linearized density-matrix as an approximation to the self-consistent GW total energy

Fabien Bruneval,¹ Mauricio Rodriguez-Mayorga,¹ Patrick Rinke,² and Marc Dvorak²

¹*Service de Recherches de Métallurgie Physique, CEA, Université Paris-Saclay, F-91191 Gif-sur-Yvette, France*

²*Department of Applied Physics, Aalto University School of Science, 00076-Aalto, Finland*

(Dated: 26 November 2020)

The linearized GW density matrix (γ^{GW}) is an efficient method to improve the static portion of the self-energy compared to ordinary G_0W_0 while keeping the single-shot simplicity of the calculation. Previous work has shown that γ^{GW} gives an improved Fock operator and total energy components that approach self-consistent GW quality. Here, we test γ^{GW} for dimer dissociation for the first time by studying N_2 , LiH , and Be_2 . We also calculate a set of self-consistent GW results in identical basis sets for a direct and consistent comparison. γ^{GW} approaches self-consistent GW total energies for a starting point based on a high amount of exact exchange. We also compare the accuracy of different total energy functionals, which differ when evaluated with a non-self-consistent density or density matrix. While the errors in total energies among different functionals and starting points are small, the individual energy components show noticeable errors when compared to reference data. The energy component errors of γ^{GW} are smaller than functionals of the density and we suggest that the linearized GW density matrix is a route to improving total energy evaluations in the adiabatic connection framework.

I. INTRODUCTION

The GW approximation to the many-electron problem¹ earned its reputation as a successful method for solids with accurate band structure predictions.²⁻⁵ Despite its development in the 1960's and early considerations in the context of propagator theory⁶, GW has only recently gained popularity in chemistry for its accurate predictions of orbital energies.⁷⁻²⁰ A lesser known fact is that GW is also a ground state theory since the total energy can be obtained from the Green's function.²¹⁻²⁴ The GW total energy and the closely related Random-Phase Approximation (RPA) energy capture non-local correlation effects, such as the van der Waals interactions,²⁵⁻³¹ which makes them attractive as advanced exchange-correlation functionals in density-functional theory (DFT) or Green's function methods.

The GW equations are meant to be solved self-consistently as the solution to Dyson's equation. In practice, self-consistent solutions are still rare, though increasing in frequency. A non-self-consistent evaluation of the self-energy based on a mean-field Green's function is much more common and far less computationally expensive. As a compromise, one of us recently introduced the linearized GW density matrix, denoted γ^{GW} .^{32,33} γ^{GW} is evaluated in a single-shot way, as with G_0W_0 , but its off-diagonal elements give an update to the static portion of the self-energy that is not accessible with ordinary G_0W_0 . Initial calculations show that the resulting total energies are in better agreement with reference data than ordinary G_0W_0 .

To develop a better understanding of Green's-function-based total energy methods, systematic tests are required. However, such systematic benchmarking is met by several challenges. The first challenge is concep-

tual. Many nonequivalent total energy functionals of the Green's function have been proposed, e.g., RPA (or Klein functional),³⁴ Luttinger-Ward,³⁵ or Galitskii-Migdal³⁶ (GM), that only agree for the fully self-consistent G . The simple one-shot procedure, which is commonly used, is therefore problematic as it leads to functional dependent GW total energies. In the 2000's, GW total energy functionals were investigated that can be evaluated with a one-shot Green's function G_0 and still retain some similarity with the fully self-consistent result.³⁷⁻⁴¹ Furthermore, we notice that today adiabatic-connection total energies are experiencing a renewed interest.⁴²⁻⁴⁴ These methods go beyond GW in terms of Feynman diagrams. However, in most cases, they are implemented in a non-self-consistent fashion. A careful assessment of their performance for non-self-consistent Green's functions is therefore timely and valuable.

The second challenge relates to conservation laws that could be violated when using a one-shot procedure. For example, the electron number is not conserved in non-self-consistent GW calculations^{45,46}. A loss or surplus of electrons leads to large changes in the electrostatic repulsion energy (Hartree energy) and subsequent total energy errors. Conversely, self-consistent GW calculations based on the Dyson equation obey the conservation laws by construction.

The last challenge involves benchmarking data. Ideally, we would test non-self-consistent total energy methods against fully self-consistent GW calculations. However, such fully self-consistent GW calculations are a numerical challenge of their own and thus rare in the literature.^{24,40,46-50} Owing to the slow basis set convergence of GW total energy methods, all benchmarking calculations should be performed with the same basis sets. This requirement aggravates systematic benchmarking

considerably, since almost all self-consistent GW reference studies employ different basis sets.

In this work, we assess the accuracy of different total energy functionals for dimer dissociation with emphasis on the performance of the linearized GW density matrix. Recognizing the difficulty of obtaining unambiguous self-consistent GW (sc GW) data, we also perform our own sc GW calculations in identical basis sets for a consistent comparison. We reach a complete picture of the performance of one-shot GW total energies, the linearized GW density matrix, and their starting point dependencies for the evaluation of total energies in critical dissociation problems. Our results allow us to perform a detailed energy component analysis on the performance of the various methods. We conclude that γ^{GW} corrects some of the error in energy components that appears in energy evaluations based on the non-self-consistent Green's function. γ^{GW} therefore shows promise as an improved single-shot total energy method.

This article is organized as follows: In Section II, we recap the different energy expressions that can be used in the context of GW total energies: sc GW , RPA, and linearized GW density-matrix. We derive an analytic proof of the electron conservation of the latter. In Section III, we describe the critical steps and settings to obtain the numerical results. Then, studying molecular bond dissociations, we address the quality of the different functionals as compared to self-consistent GW in Section IV. The approximations of one-shot adiabatic-connection calculations are explored in the final results section, Section V. Conclusions are given in Section VI. Hartree atomic units are used everywhere in the manuscript. Real wave functions are assumed.

II. GW TOTAL ENERGIES

A. Many-body perturbation theory

Many-body perturbation theory considers the Green's function G as its central object.⁵¹ The single-particle Green's function is

$$G(\mathbf{r}, \mathbf{r}', t - t') = -i \langle N | \hat{T} [\hat{\psi}(\mathbf{r}, t) \hat{\psi}^\dagger(\mathbf{r}', t')] | N \rangle \quad (1)$$

for field creation (annihilation) operator $\hat{\psi}^\dagger(\mathbf{r}')$ ($\hat{\psi}(\mathbf{r})$), time-ordering operator \hat{T} , and ground state $|N\rangle$ (we suppress spin variables). The Green's function contains a great deal of information. For instance, at time zero the Green's function yields the so-called one-particle reduced density matrix:

$$\gamma(\mathbf{r}, \mathbf{r}') = -iG(\mathbf{r}, \mathbf{r}', 0^-), \quad (2)$$

where 0^- stands for the left-hand-side limit to time 0 (t' is infinitesimally later than t , $t' \rightarrow t^+$). Going even further, contracting the spatial indices yields the electronic density:

$$\rho(\mathbf{r}) = -iG(\mathbf{r}, \mathbf{r}, 0^-). \quad (3)$$

These will be useful quantities when evaluating the total energy later.

The Green's function obeys the Dyson equation

$$G = G_0 + G_0(\Sigma_{xc}[G] - v_{xc})G. \quad (4)$$

The Dyson equation connects a non-interacting Green's function G_0 obtained with the exchange-correlation potential v_{xc} ⁵² to the fully interacting Green's function G that corresponds to the self-energy Σ_{xc} . Space and time variables have been omitted for simplicity. Equation 4 is perhaps the best way to explain the self-energy, as the connection between G_0 and G . The self-energy itself is a functional of G and therefore the Dyson equation must be solved self-consistently.

Here, we focus on the GW approximation to the self-energy. By subtracting the bare Coulomb interaction v , which gives rise to the exact-exchange operator Σ_x , we obtain the correlation part of the self-energy, Σ_c , that reads in the GW approximation^{1,53}

$$\Sigma_c(\mathbf{r}, \mathbf{r}', t - t') = iG(\mathbf{r}, \mathbf{r}', t - t') \times [W(\mathbf{r}, \mathbf{r}', t - t') - v(\mathbf{r} - \mathbf{r}')], \quad (5)$$

with W , the screened Coulomb interaction. The GW approximation obviously depends on the Green's function G and therefore should be calculated self-consistently to satisfy the Dyson equation, in theory. But as the expression shows, Σ_c is dynamic and non-local, which makes the self-consistent calculations numerically involved. It is then very tempting to skip the self-consistency and evaluate the GW self-energy only once using a generalized Kohn-sham Green's function G_0 .

The self-consistent GW approach has a major advantage over non-self-consistent calculations, which is that it conserves particle number. sc GW is conservative according to the Baym-Kadanoff criterium:⁵⁴ The GW self-energy can be formally obtained from a functional derivative of a correlation functional with respect to G . This ensures that the density calculated from the resulting Green's function conserves the number of electrons.

B. Self-consistent GW energies with Galitskii-Migdal

A general way of calculating the total energy from the Green's function is with the Galitskii-Migdal formula,

$$E_{\text{total}}^{\text{GM}}[G] = T[G] + V_{ne}[G] + E_H[G] + E_x[G] + E_c[G] + V_{nn} \quad (6)$$

for kinetic energy T , external potential energy V_{ne} , Hartree energy E_H , exchange energy E_x , correlation energy E_c , and nuclei repulsion V_{nn} . All of these energy components are functionals of the Green's function and can be evaluated with any given candidate G .

However, only the correlation energy itself actually depends on the full dynamical Green's function $G(\mathbf{r}, \mathbf{r}', t -$

t'). All the other components just need the time zero Green's function. For instance, let us show this statement for the kinetic energy, whose definition as a functional of G reads⁵⁵

$$T[G] = -i \int d\mathbf{r} \lim_{t' \rightarrow t^+} \lim_{\mathbf{r}' \rightarrow \mathbf{r}} \left(-\frac{\nabla_{\mathbf{r}}^2}{2} \right) G(\mathbf{r}, \mathbf{r}', t - t'). \quad (7)$$

The kinetic operator $-\nabla_{\mathbf{r}}^2/2$ does not act on the time variables so that the limit $t' \rightarrow t^+$ and the kinetic operator can be swapped. With this, the kinetic energy becomes an explicit functional of the sole one-particle reduced density matrix γ introduced in Eq. (2):

$$T[\gamma] = \int d\mathbf{r} \lim_{\mathbf{r}' \rightarrow \mathbf{r}} \left(-\frac{\nabla_{\mathbf{r}}^2}{2} \right) \gamma(\mathbf{r}, \mathbf{r}'). \quad (8)$$

Similar arguments can be used to demonstrate that the exchange energy is also a functional of γ :

$$E_x[\gamma] = -\frac{1}{2} \int d\mathbf{r} \int d\mathbf{r}' \gamma(\mathbf{r}, \mathbf{r}') \frac{1}{|\mathbf{r} - \mathbf{r}'|} \gamma(\mathbf{r}', \mathbf{r}) \quad (9)$$

and that the electrostatic energies V_{ne} and E_H are functionals of the even simpler electronic density $\rho(\mathbf{r})$.

To summarize these remarks, we explicitly introduce γ and ρ in the Galitskii-Migdal total energy expression introduced in Eq. (6):

$$E_{\text{total}}^{\text{GM}}[G] = T[\gamma] + V_{ne}[\rho] + E_H[\rho] + E_x[\gamma] + E_c[G] + V_{nn}. \quad (10)$$

Our total energy calculations based on scGW follow this Galitskii-Migdal procedure. Just the correlation energy $E_c[G]$ is not defined yet. The general correlation energy in the Galitskii-Migdal formalism is

$$E_c[G] = \frac{1}{2} \int_{-\infty}^{\infty} \frac{d\omega}{2\pi} \text{Tr}\{G(\mu + i\omega)\Sigma_c(\mu + i\omega)\}, \quad (11)$$

where the Tr operator implies an integral over the spatial coordinates. In the previous expression, we have introduced the Fourier transform of the correlation self-energy Σ_c and of the Green's function G for imaginary frequencies $\mu + i\omega$ with μ a real-valued energy that separates occupied and empty electronic states. Our own Galitskii-Migdal energies are numerically evaluated with Eq. 11.

The correlation energy can be transformed in an equivalent expression that is numerically simpler and more similar to the adiabatic-connection correlation energy as we will see. Let us introduce in Eq. (11) the irreducible polarizability $\chi_0 = -iGG$, the GW correlation self-energy from Eq. (5), the expression of the screened Coulomb interaction $W = v + v\chi v$ as a function of the reducible polarizability $\chi = \chi_0 + \chi_0 v\chi$ to obtain

$$E_c[G] = \frac{1}{2} \int_{-\infty}^{\infty} \frac{d\omega}{2\pi} \text{Tr}\{v\chi_0(i\omega) - v\chi(i\omega)\}. \quad (12)$$

Eq. 12 is the Galitskii-Migdal correlation energy in the GW approximation.

In practical calculations, GW total energies are known to precisely capture the correlation energy of the homogeneous electron gas.^{22,23,37,48} However, the correlation energy is found to be too negative for molecules.^{24,41} Higher-order terms are necessary to fix this shortcoming.⁵⁶

C. Non-self-consistent Klein functional or random-phase approximation

As the self-consistent evaluation of the GW self-energy and Green's function is very challenging, it is common to use single-shot calculations of G when evaluating the total energy. This introduces both a dependence on the mean-field starting point *and* a dependence on the choice of energy functional. As mentioned previously, different expressions for the total energy do not agree for non-self-consistent Green's functions.

The most widely used approximation in this context is certainly the Klein functional³⁴ and its DFT counterpart, RPA. The Klein functional is obtained from the adiabatic connection of a non-interacting and a fully interacting system with the same (exact) electronic density. The Hohenberg-Kohn theorem⁵⁷ guarantees that a local potential that produces the exact density can always be found irrespective of the Coulomb interaction strength λ .

Hence, with this constant density, the different components of the total energy can be integrated over the coupling constant λ from zero (non-interacting electrons) to one (fully interacting electrons). The obtained expression contains functionals with logarithms of the self-energy, which would be rather difficult to evaluate for general Green's functions G and is of no use to us here (See Appendix B of Ref. 40, for instance).

However, the Klein functional simplifies much when evaluated with a Green's function G_0 produced from a one-electron self-consistent field (SCF). In this case, G_0 reads

$$G_0(\mathbf{r}, \mathbf{r}', \omega) = 2 \sum_n \frac{\varphi_n(\mathbf{r})\varphi_n^*(\mathbf{r}')}{\omega - \epsilon_n \pm i\eta}, \quad (13)$$

where $\varphi_n(\mathbf{r})$ and ϵ_n are the eigenfunctions and eigenvalues obtained for the SCF. η is a vanishing positive real number. Then the Klein functional becomes³⁹

$$E_K[G_0] = T_s[\varphi] + V_{ne}[\rho^{\text{SCF}}] + E_H[\rho^{\text{SCF}}] + E_x[\varphi] + \Phi_c[G_0] + V_{nn}, \quad (14)$$

where we stress with the notation $T_s[\varphi]$ that the kinetic energy is evaluated with Kohn-Sham orbitals and hence does not contain the correlation part of the kinetic energy. The SCF density is denoted ρ^{SCF} .

Finally, the correlation functional $\Phi_c[G_0]$ introduced in Eq. (14) is identical to the one coined RPA in the framework of the adiabatic-connection fluctuation-dissipation

approach to DFT:⁵⁸

$$\Phi_c[G_0] = \frac{1}{2} \int_{-\infty}^{\infty} \frac{d\omega}{2\pi} \text{Tr} \{v\chi_0(i\omega) + \ln[1 - v\chi_0(i\omega)]\}. \quad (15)$$

In this work, energies denoted RPA are calculated with Eqs. 14 and 15. Notice the differences and similarities between the correlation energy functionals E_c defined in Eq. (12) and Φ_c defined in Eq. (15). The difference between Φ_c and E_c is usually interpreted as the kinetic correlation energy that Φ_c should contain whereas E_c should not.

In non-self-consistent calculations, the RPA functional and the Klein functional give the same total energy. However, the agreement is lost at self-consistency.⁴⁷ Remember that the RPA functional is defined in the framework of Kohn-Sham DFT and that the self-consistent cycles are performed to obtain a *local* Kohn-Sham potential. The Klein functional is a Green's function approach and will converge to the self-consistent *GW* result. As the vast majority of the practical cases use a non-self-consistent approach, we will consider RPA or Klein functional as synonyms in the following.

D. Linearized *GW* density matrix

Recently, the linearized *GW* density-matrix (γ^{GW}) was introduced. It provides a third option to compute the total energy in our study, the other two being Galitskii-Migdal and the Klein functional.^{32,33} This density matrix is obtained from the linearized Dyson equation

$$G = G_0 + G_0(\Sigma_{xc}[G_0] - v_{xc})G_0, \quad (16)$$

where all Green's functions G on the right-hand side of the equation have been replaced with a non-interacting G_0 . This linear approximation is customary in the context of the Sham-Schlüter equation,^{59,60} where a local potential is derived from a non-local dynamical self-energy.

The linearized *GW* density matrix has several interesting properties, despite the fact that it is obtained from a linearized approximation. First, γ^{GW} has a closed expression in the Kohn-Sham orbital basis:

$$\gamma_{ij}^{GW} = 2\delta_{ij} - 2 \sum_{as} \frac{w_{ia}^s w_{ja}^s}{(\epsilon_i - \epsilon_a - \Omega_s)(\epsilon_j - \epsilon_a - \Omega_s)} \quad (17a)$$

$$\gamma_{ab}^{GW} = 2 \sum_{is} \frac{w_{ai}^s w_{bi}^s}{(\epsilon_i - \epsilon_a - \Omega_s)(\epsilon_i - \epsilon_b - \Omega_s)} \quad (17b)$$

$$\begin{aligned} \gamma_{ib}^{GW} = & 2 \frac{\langle i | \Sigma_x - v_{xc} | b \rangle}{\epsilon_i - \epsilon_b} \\ & + 2 \frac{1}{\epsilon_i - \epsilon_b} \left[\sum_{as} \frac{w_{ia}^s w_{ba}^s}{(\epsilon_i - \epsilon_a - \Omega_s)} \right. \\ & \left. - \sum_{js} \frac{w_{ij}^s w_{bj}^s}{(\epsilon_j - \epsilon_b - \Omega_s)} \right], \quad (17c) \end{aligned}$$

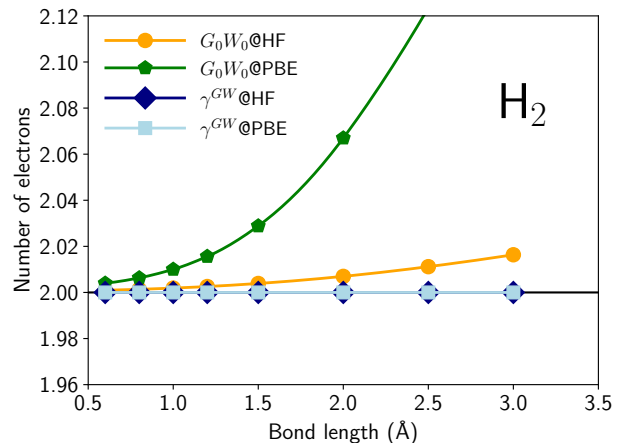


FIG. 1. Number of electrons as a function of the bond length in H_2 for different approximations. G_0W_0 stands for a one-shot evaluation of the Dyson equation, whereas γ^{GW} stands for the linearized *GW* density-matrix. Calculations are performed in aug-cc-pV5Z basis set.

where i, j indices run over occupied orbitals and a, b over empty orbitals. The virtual-occupied terms γ_{bi}^{GW} can be readily obtained thanks to the symmetry of the density matrix. The poles Ω_s and the residues w^s of the reducible polarizability $v\chi v$ can be obtained analytically^{61–63} solving Casida-like equations.^{64,65} A detailed derivation and the generalization of spin-unrestricted case for these equations can be found in Ref. 33.

Second, the linearized *GW* density matrix conserves the number of electrons, which is not the case for regular non-self-consistent Green's functions. The number of electrons is obtained from the trace of γ^{GW} , which we can perform analytically by considering the diagonal terms in Eqs. (17a)-(17c):

$$\begin{aligned} \text{Tr}\gamma^{GW} &= \sum_i \gamma_{ii}^{GW} + \sum_{a\sigma} \gamma_{aa\sigma}^{GW} \\ &= \sum_i 2\delta_{ii} = N. \end{aligned} \quad (18)$$

We have used the symmetry $w_{ia}^s = w_{ai}^s$ to arrive at the final result.

In Fig. 1, we illustrate the gain of electrons with ordinary G_0W_0 and conservation of electrons with γ^{GW} by studying the stretched H_2 molecule. The one-shot Dyson equation is solved numerically for imaginary frequencies. The Hartree-Fock (HF) based G_0 reproduces earlier calculations and gives a relatively small error.^{41,66} Conversely, for PBE-based G_0W_0 calculations, the electron number is already too high at equilibrium and then increases further as the hydrogen atoms move apart from each other. As expected from the formal derivation in Eq. (18), the linearized density-matrix γ^{GW} always perfectly conserves the number of electrons, irrespective of the SCF starting point.

Finally, we propose an alternative expression for the total energy that equals the scGW total energy when evaluated with a self-consistent Green’s function³³

$$E_{\text{total}}^{\gamma^{GW}} = T[\gamma^{GW}] + V_{ne}[\rho^{GW}] + E_H[\rho^{GW}] + E_x[\gamma^{GW}] + E_c[G_0] + V_{nn}. \quad (19)$$

In Eq. (19), the correlation energy E_c is the Galitskii-Migdal expression shown in Eq. (12) but evaluated with a non-interacting Green’s function G_0 . This expression is different from the correlation energy of the RPA/Klein functional (Φ_c) in that it does not include the kinetic correlation energy, which is already included in the kinetic energy term $T[\gamma^{GW}]$. As a side note we like to reiterate that γ^{GW} is a correlated density matrix with occupation numbers that depart from 0 or 1 (non-idempotency). In previous work, one of us has shown that the occupation numbers of γ^{GW} approximate those obtained from scGW for the stretched H_2 molecule.³³

Now we need to evaluate the different total energy expressions for realistic molecules. We first present in the following sections the technical details for the numerical implementations.

III. GW TOTAL ENERGIES IN GAUSSIAN BASIS WITH MOLGW AND FHI-AIMS

To compare the different total energy expressions in practice, we have used two computer codes that have GW capabilities for molecules, namely MOLGW⁶³ and FHI-AIMS.^{11,67} Both codes can use the same Gaussian basis sets. Nevertheless, some important technical details vary.

MOLGW uses analytic Gaussian-type orbitals, as is customary in quantum chemistry. With this choice of orbitals, the integrals in the Hamiltonian can be evaluated analytically with recursive formulas.^{68,69} FHI-AIMS uses numeric atomic-centered orbitals. This approach is more versatile as any type of atomic-centered orbital can be used, in principle. However, the integrals have to be computed using a quadrature.⁶⁷ In the present study, we employ spherical Gaussian orbitals from the Dunning family.⁷⁰ The discretization and quadrature errors in FHI-AIMS are known to be negligible. We use the same settings for the basis and numerical quadrature as determined in Ref. 71 for Gaussian-type orbitals in FHI-AIMS.

Both codes use the resolution of the identity approximation in order to eliminate the two-electron 4-center repulsion integrals.^{72,73} This approximation has been shown to be extremely efficient and accurate for the GW self-energy.^{9,11,74} In MOLGW and FHI-AIMS, an atomic-centered auxiliary basis is introduced to split the 4-center integrals into 2-center and 3-center integrals using the so-called Coulomb metric. For our present purpose of total energy comparisons, we have used much more complete auxiliary basis sets than usually needed

for GW orbital energies. In MOLGW, we have used the “PAUTO” recipe as described in Ref. 75 and implemented in GAUSSIAN.⁷⁶ This technique automatically generates an auxiliary basis set corresponding to an input basis set. Its accuracy in the context of GW calculations has already been assessed in Ref. 77. In FHI-AIMS, the RI basis is initialized with all possible on-site products of the chosen numeric atomic-centered orbitals which, in this work, are the Gaussian-type orbitals. The set of these auxiliary basis functions centered on a chosen atomic site are reduced with a Gram-Schmidt-like orthogonalization procedure. FHI-AIMS further reduces the auxiliary basis through a singular value decomposition to orthogonalize auxiliary basis functions centered on different atoms.

In Table I, we show the HF total energy at the micro-Hartree accuracy for three systems: the helium atom, the neon atom, and ethene (C_2H_4). The error induced by the two different auxiliary bases can be measured by the difference in their HF energies. It is always lower than 0.1 mHa, which is more than sufficient for all the results that will be reported in the following.

Finally, the two codes treat the GW self-energy differently. In scGW calculations, FHI-AIMS fits all dynamical quantities needed for the self-consistent calculation on an additional auxiliary basis of Lorentzians in order to perform Fourier transforms analytically.⁷⁸ As shown in Eq. (12), the Green’s function $G(\mu+iu)$ is only needed for imaginary frequencies to calculate the correlation energy. The same statement holds for the density and the density matrix entering the other parts of the energy expression in Eq. (10). As a consequence, the entire total energy can be evaluated from the sole knowledge of $G(\mu+iu)$ at the expense of a quadrature on the imaginary axis. FHI-AIMS uses an exponentially spaced imaginary frequency grid so that grid point k is placed at

$$\omega_k = \omega_0[e^{(k-1)h} - 1] \quad (20)$$

for a constant h that determines the maximum frequency. Our calculations are converged with 60 frequency points, in agreement with previous convergence studies.⁷⁸

MOLGW takes an alternative route to calculating the self-energy, as it is mostly devoted to “one-shot” calculations. When a non-interacting Green’s function G_0 is used, a simple spectral decomposition of the self-energy can be obtained, as shown in Ref. 63, but at the expense of a large diagonalization. With this spectral decomposition, the correlation energy is calculated analytically.

The “one-shot” GM G_0W_0 correlation energy based on a HF starting point computed with both codes is given in Table I for the same three electronic systems. The difference between FHI-AIMS and MOLGW quantifies the quadrature error. In all cases, the error remains well below 0.1 mHa. In the end, the GM total energy $E_{\text{total}}^{\text{GM}}$, which is the sum of the two previous columns, varies very little when comparing the two codes. Therefore, we have verified the consistency of the results obtained with MOLGW and FHI-AIMS.

TABLE I. Hartree-Fock, G_0W_0 @HF GM correlation and total energies in cc-pVQZ basis obtained in FHI-AIMS and MOLGW codes (Ha).

	HF	$E_c[G_0]$	$E_{\text{total}}^{\text{GM}}$
He			
FHI-AIMS	-2.861514	-0.120551	-2.982065
MOLGW	-2.861514	-0.120554	-2.982068
Diff.	2.3×10^{-7}	2.5×10^{-6}	2.7×10^{-6}
Ne			
FHI-AIMS	-128.543452	-0.759737	-129.303189
MOLGW	-128.543470	-0.759780	-129.303250
Diff.	1.8×10^{-5}	4.4×10^{-5}	6.1×10^{-5}
C_2H_4			
FHI-AIMS	-78.068893	-0.997408	-79.066301
MOLGW	-78.068823	-0.997380	-79.066203
Diff.	7.0×10^{-5}	2.8×10^{-5}	9.8×10^{-5}

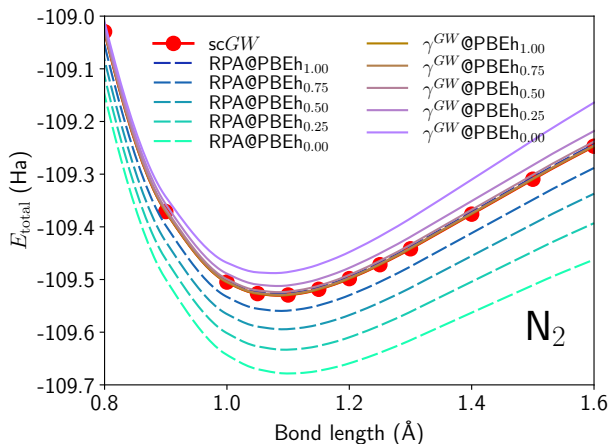


FIG. 2. N_2 dissociation curve obtained with scGW and different one-shot evaluations in cc-pVQZ basis. RPA or Klein functional total energies are shown with dashed lines. Linearized GW total energies are shown with solid lines.

IV. DISSOCIATION CURVES

We can now evaluate the performance of the different GW total energies for realistic situations. Diatomic molecules are very often considered as a benchmark for computational chemistry methods. Here, we treat three molecules that have very different types of bond: N_2 , a covalently bonded molecule, LiH, an ionic molecule, and Be_2 , a van der Waals bonded dimer.

In the following, we compare the scGW total energy to the one-shot evaluations in the RPA/Klein functional, labeled RPA, or in the GM functional based on the linearized GW density-matrix, denoted γ^{GW} . As the latter two formulas are not self-consistent, they necessarily depend on the SCF approximation on which they are based.

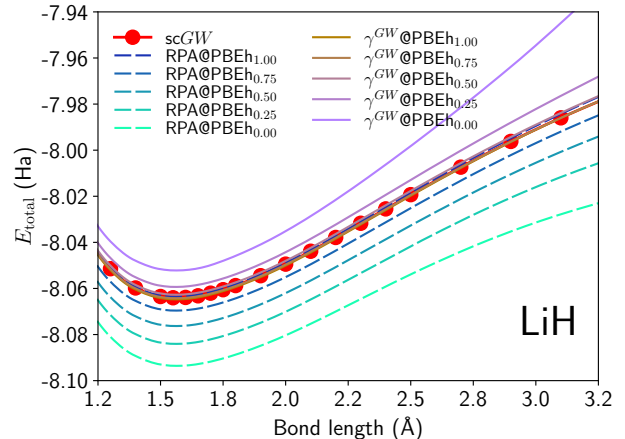


FIG. 3. LiH dissociation curve obtained with scGW and different one-shot evaluations in cc-pVQZ basis. RPA or Klein functional total energies are shown with dashed lines. Linearized GW total energies are shown with solid lines.

TABLE II. Equilibrium bond lengths in Angstrom for N_2 , LiH, and Be_2 . Below the scGW results, rows correspond to the starting self-consistent mean-field inputs, whereas columns show the two energy formulas, RPA or γ^{GW} .

	N_2		LiH		Be_2	
scGW	1.0865		1.5627		2.6567	
	RPA	γ^{GW}	RPA	γ^{GW}	RPA	γ^{GW}
PBEh _{1.00}	1.0859	1.0861	1.5604	1.5631	2.6838	2.6844
PBEh _{0.75}	1.0886	1.0861	1.5611	1.5619	2.5953	2.6773
PBEh _{0.50}	1.0914	1.0855	1.5617	1.5612	2.5328	2.6817
PBEh _{0.25}	1.0946	1.0836	1.5632	1.5580	2.4655	2.8269
PBEh _{0.00}	1.0985	1.0767	1.5674	1.5616	2.3683	3.2400

We use the notation “RPA@” and “ γ^{GW} @” to highlight the starting point dependence.

A convenient way of exploring the starting point dependence is to play with the exact-exchange content α in the PBEh hybrid functional.⁷⁹ Within this approach, the standard PBE functional⁸⁰ is denoted PBEh_{0.00} and the PBE0 functional⁸¹ PBEh_{0.25}.

Figure 2 shows the dissociation curves for the N_2 molecule. The equilibrium bond lengths are summarized in Table II. Even though all the curves have a very similar minimum, the γ^{GW} total energy is less sensitive to the starting point than RPA. For PBEh_{1.00}, both RPA and γ^{GW} agree remarkably well with the scGW curve. However, when decreasing the amount of exact-exchange, the RPA energies continuously go down. On the contrary, the γ^{GW} energies are much less sensitive to the SCF starting point and slowly go up when decreasing α .

The very same conclusions can be drawn from the analysis of LiH dissociation in Fig. 3: Both expressions agree

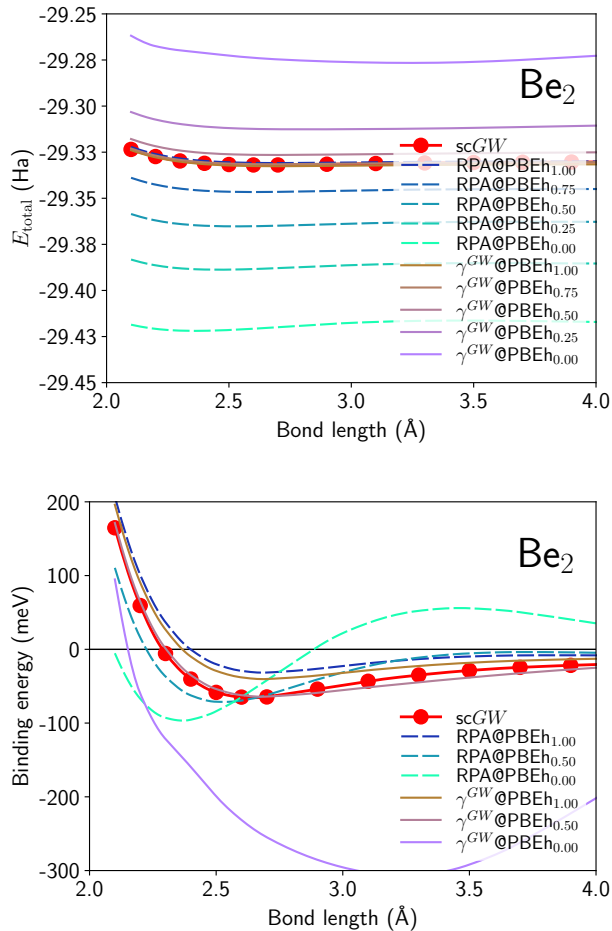


FIG. 4. Be_2 dissociation curve with scGW and different one-shot evaluations in cc-pV5Z basis (upper panel). Be_2 binding energy with scGW and different one-shot evaluations in cc-pV5Z basis (lower panel).

for $\text{PBEh}_{1.00}$, and γ^{GW} is less sensitive to the starting point than RPA. Here, for LiH, a pathological behavior of $\gamma^{GW}@PBEh_{0.00}$ can be observed: The total energy rises too rapidly as the bond length increases. The weird behavior happens in the region where the transition from an ionic bonding $\text{Li}^+ \text{H}^-$ to an atomic limit $\text{Li} \cdot \text{H} \cdot$ starts.⁸²

Then we turn to the delicate case of Be_2 , which has been carefully investigated in the past to determine the ability of the RPA functional to capture the elusive van der Waals interactions.^{83–85} Be_2 is interesting for another reason: its binding energy curve often exhibits a large positive bump at intermediate bond lengths.

The upper panel of Fig. 4 shows the total energy along the Be_2 dissociation. Again, the RPA dependence on the SCF starting point is worrying, whereas the γ^{GW} expression is much less sensitive. However, the binding energy of the beryllium dimer is so weak that it is better to inspect the binding energy curves instead, in which the energy of the two isolated beryllium atoms has been subtracted from the total energy.

The lower panel of Fig. 4 shows the binding energy curves of Be_2 . First of all, scGW produces a smooth binding energy curve with a minimum and no bump at intermediate bond lengths. This in itself is a remarkable result, which has, to our knowledge, not been reported, yet. This behavior contrasts with the huge positive bump found for $\text{RPA}@PBEh_{0.00}$ and the huge negative bump observed for $\gamma^{GW}@PBEh_{0.00}$. However when the exact-exchange amount is increased, both functionals behave much better. In particular, $\gamma^{GW}@PBEh_{0.50}$ is a very convincing approximation to scGW.

Across these dissociation curves, one can draw the general conclusion that the PBE starting point should be avoided for molecules. Additionally, hybrid functionals with a large content of exact-exchange are a better SCF starting point for both RPA and γ^{GW} in the sense that they better approach the scGW result. The γ^{GW} total energy appears less sensitive to the starting point and might be thought of as a reliable way to avoid the heavy self-consistent GW calculations.

V. ENERGY COMPONENT COMPARISON

In the previous Section, we discussed the quality of total energies in the non-self-consistent approximations to scGW. However, even when they agree, these approximations are built with different energy components. For instance, the Hartree energy in the RPA functional is constructed directly from a DFT electronic density, whereas in the γ^{GW} functional, it is obtained from the linearized GW density matrix. Even when the total energies match between RPA, γ^{GW} and scGW, it is very much possible that the individual components of the total energy differ.

In our study, the individual parts of the scGW total energy are available, which provides us with a unique opportunity to appraise the quality of each component of the total energy. This analysis is instructive not only for the approximation to the GW total energy itself, but for the general framework of adiabatic-connection fluctuation-dissipation (ACFD). Indeed, the vast majority of the ACFD approaches rely on a non-self-consistent calculation, in which the electronic density is kept constant and equal to the underlying SCF starting point.

In this section, we consider the examples of water and methane, whose energy components are shown in Figs. 5 and 6. In these series of plots, we provide the total energy, the kinetic energy, the electron-nucleus energy, the Hartree energy, the exchange energy, and the sum of the latter three as a function of the starting SCF method. To span a wide range of starting points, we give the results for all the tuned PBEh functionals from $\alpha = 0$ to $\alpha = 1$ and also for pure HF. As reference, we also provide the scGW and the coupled-cluster (CCSD) results. The latter ones have been calculated with Gaussian16.⁷⁶ Note that for comparison purposes, we have enforced the same energy scale on the y-axis and the data sometimes fall outside the graph.

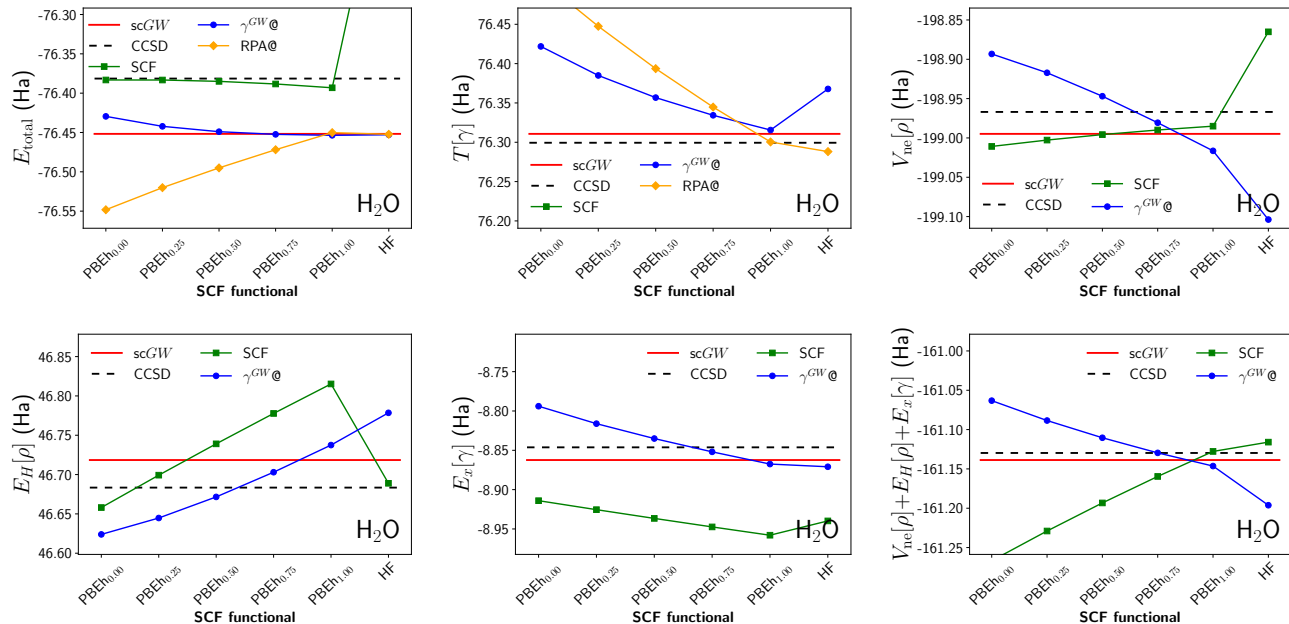


FIG. 5. H_2O energy decomposition as a function of the starting SCF functional in cc-pVQZ basis. Energy parts are given for SCF, RPA, γ^{GW} , scGW, and CCSD. Results for scGW and CCSD are independent from the starting point. Upper left panel is the total energy, upper central panel the kinetic energy, and upper right panel the electron-nucleus energy. Lower left panel is the Hartree energy, lower central panel the exchange energy, and lower right the sum of electron-nucleus, Hartree and exchange energies.

The upper left panels of Fig. 5 and 6 represent the total energy of H_2O and CH_4 . They confirm the previous conclusions: γ^{GW} reproduces quite well the scGW total energy irrespective of the starting point. RPA is more sensitive to the starting point, but with high amounts of exact exchange in the starting point both RPA and γ^{GW} reproduce the scGW total energy well. We also see that the scGW total energy is too low compared to CCSD.

Turning to the kinetic energy $T[\gamma]$ in the upper central panels of Fig. 5 and 6, the explanation requires some additional details. scGW, CCSD, and γ^{GW} methods give direct access to the reduced density matrix and therefore the kinetic energy can be calculated directly. This kinetic energy readily incorporates the so-called correlation part of the kinetic energy. The SCF kinetic energy is calculated from the Kohn-Sham orbitals and misses this correlation part. This explains why the SCF kinetic energies are way too low and the curve does not even appear on the graph. Finally, the RPA kinetic energy is defined indirectly:

$$T^{\text{RPA}} = T_s[\varphi_i] + E_c[G_0] - \Phi_c[G_0], \quad (21)$$

as the adiabatic-connection in $\Phi_c[G_0]$ is meant to capture the pure correlation energy together with the kinetic energy correlation. From the upper central panels of Figs. 5 and 6, we observe that both RPA and γ^{GW} kinetic energies are very sensitive to the starting SCF functional.

For the next energies in Figs. 5 and 6, namely the

electron-nucleus V_{ne} , Hartree E_H , and exchange E_x energies, the RPA values are identical to the SCF energies in the “one-shot” approach. For the other methods, one can first note the astonishing agreement of those energies within scGW and CCSD. Then, both RPA and γ^{GW} energies are rather sensitive to the chosen starting point.

However, the different deviations may compensate to some extent. Let us quantify this with the lower right panels of Figs. 5 and 6. There we draw the sum $V_{\text{ne}} + E_H + E_x$ that is not updated in a “one-shot” adiabatic-connection approach. For the SCF calculations alone, a large amount of exchange is required to match scGW or CCSD for H_2O , whereas for CH_4 SCF always remains too low. Conversely, γ^{GW} agrees well with scGW and CCSD for large amounts of exchange for both molecules.

We conclude that the “one-shot” adiabatic-connection approach can be problematic since simple parts of the total energy, such as the electrostatic and the exchange components, are kept unchanged and equal to their SCF starting point. Hence, improving the adiabatic connection total energy would imply compensating the “one-shot” error with the correlation energy. This could, in turn, worsen the correlation energy component by itself. Working with an improved density matrix, such as $\gamma@PBEh_{0.75}$ would accurately separate the necessary improvement to the correlation energy from the improvement to the electrostatic and exchange energies. Com-

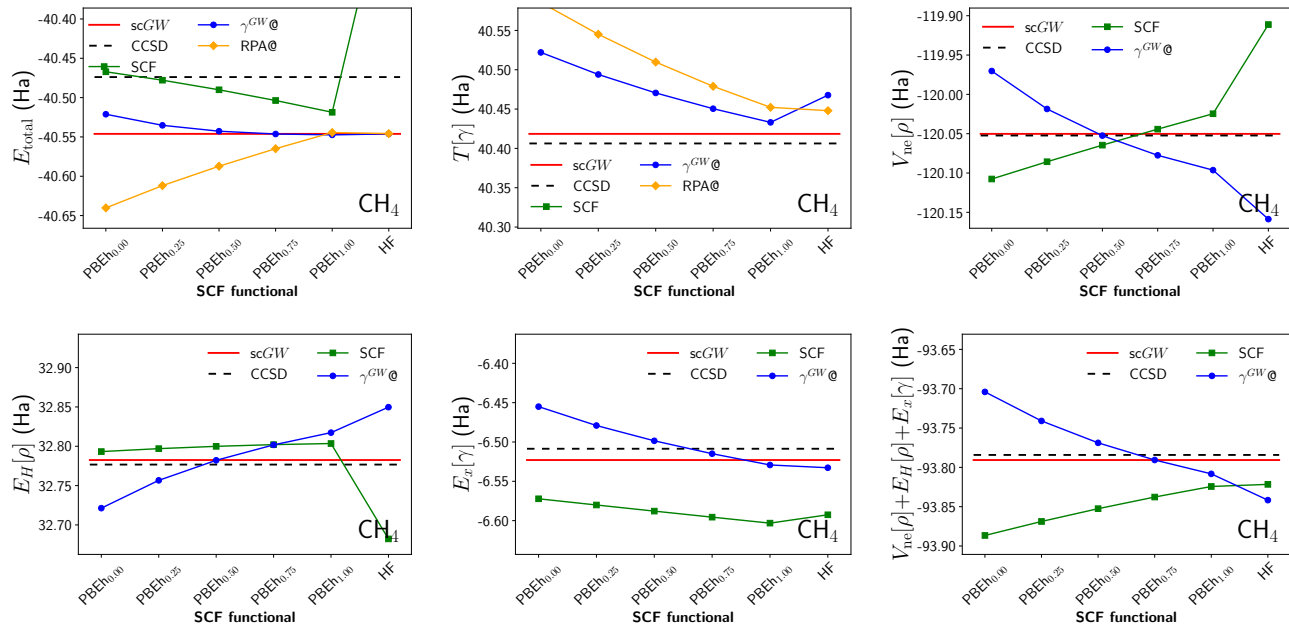


FIG. 6. CH_4 energy decomposition as a function of the starting SCF functional in cc-pVQZ basis. Energy parts are given for SCF, RPA, γ^{GW} , scGW, and CCSD. Results for scGW and CCSD are independent from the starting point. Upper left panel is the total energy, upper central panel the kinetic energy, and upper right panel the electron-nucleus energy. Lower left panel is the Hartree energy, lower central panel the exchange energy, and lower right the sum of electron-nucleus, Hartree and exchange energies.

pared with scGW and CCSD, γ @PBEh0.75 gives good total energies and total energy components.

VI. CONCLUSION

In this article, we have compared the performance of approximated GW total energy functionals to the self-consistent reference value. We have especially studied the RPA functional (also named Klein functional) and the recently proposed linearized density matrix total energy. We have shown analytically and numerically that the linearized GW density matrix conserves the number of electrons, an important property which is violated by the usual one-shot Dyson equation.

We have shown that the linearized density-matrix total energy is less sensitive to the starting SCF functional than the regular RPA when studying dissociation of diatomic molecules, including the famously difficult example of Be_2 . Both RPA and γ^{GW} total energies better approach scGW when starting from hybrid functionals with a high content of exact-exchange (0.75-1.00). This gives us a hint that those SCF functionals produce Green's functions which are reasonably close to that obtained with scGW.

With a term by term comparison of the total energy components for water and methane, we have appraised the intrinsic error introduced when performing a one-shot adiabatic-connection calculation. In one-shot cal-

culations, the electron-nucleus, the Hartree and the exchange energies are kept equal to the SCF starting point. For methane, we show that no simple hybrid functional correctly produces these energy components and no error cancellation occurs in their sum, which is not accurate when compared to the reference data. Therefore, the error in these energies permeates up to the final total energy. These findings show that the quest for a better adiabatic-connection correlation energy should come along with a quest for a better density matrix. The linearized GW density matrix may be a rung towards achieving that goal.

ACKNOWLEDGMENTS

FB and MRM acknowledge the financial support of the Cross-Disciplinary Program on Numerical Simulation of CEA, the French Alternative Energies and Atomic Energy Commission. This work was performed using HPC resources from GENCI-TGCC and GENCI-IDRIS (Grant 2020-gen6018). MD was supported by the Academy of Finland through grant no. 316347 and acknowledges the CSC – IT Center for Science, Finland, and the Aalto Science-IT project for computational resources.

¹L. Hedin, “New method for calculating the one-particle green’s function with application to the electron-gas problem,” *Phys. Rev.* **139**, A796–A823 (1965).

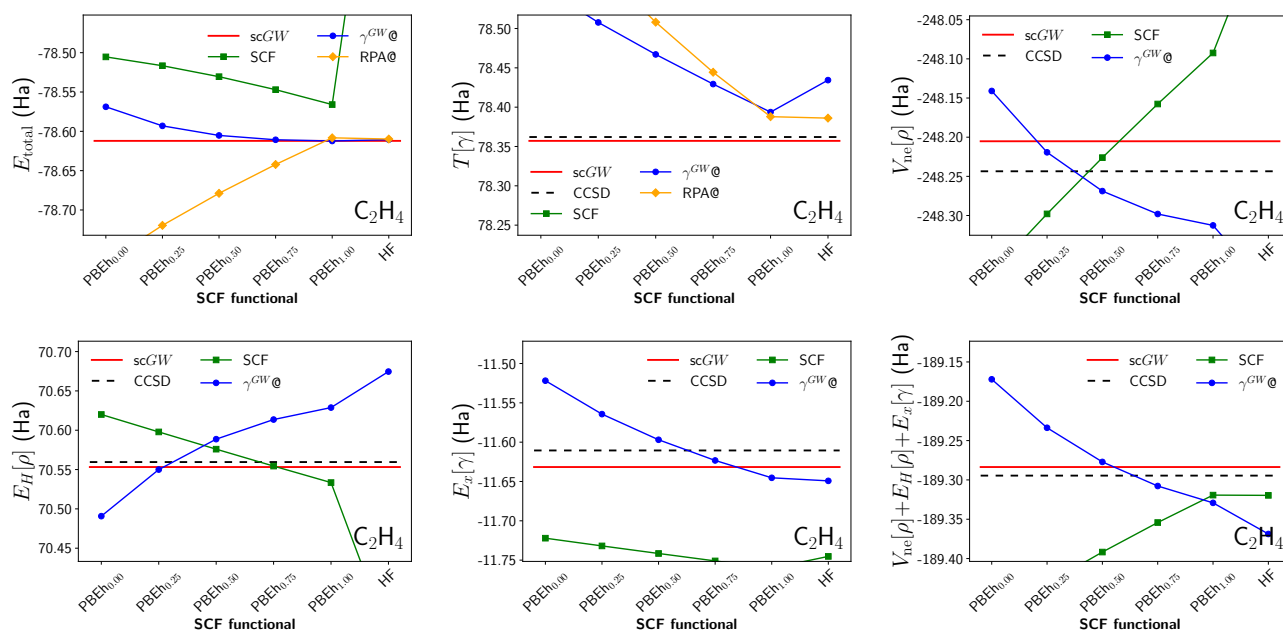


FIG. 7. C_2H_4 energy decomposition as a function of the starting SCF functional in cc-pVQZ basis. Energy parts are given for SCF, RPA, γ^{GW} , scGW, and CCSD. Results for scGW and γ^{GW} are independent from the starting point. Upper left panel is the total energy, upper central panel the kinetic energy, and upper right panel the electron-nucleus energy. Lower left panel is the Hartree energy, lower central panel the exchange energy, and lower right the sum of electron-nucleus, Hartree and exchange energies.

- ²F. Aryasetiawan and O. Gunnarsson, “The gw method,” Rep. Prog. Phys. **61**, 237–312 (1998).
- ³D. Golze, M. Dvorak, and P. Rinke, “The gw compendium: A practical guide to theoretical photoemission spectroscopy,” Frontiers in Chemistry **7**, 377 (2019).
- ⁴F. Bruneval and M. Gatti, “Quasiparticle self-consistent gw method for the spectral properties of complex materials,” in *First Principles Approaches to Spectroscopic Properties of Complex Materials*, edited by C. Di Valentin, S. Botti, and M. Cococcioni (Springer Berlin Heidelberg, Berlin, Heidelberg, 2014) pp. 99–135.
- ⁵L. Reining, “The gw approximation: content, successes and limitations,” WIREs Computational Molecular Science **8**, e1344 (2018), <https://onlinelibrary.wiley.com/doi/pdf/10.1002/wcms.1344>.
- ⁶L. S. Cederbaum and W. Domcke, “Theoretical Aspects of Ionization Potentials and Photoelectron Spectroscopy: A Green’s Function Approach,” in *Advances in Chemical Physics*, edited by I. Prigogine and S. A. Rice (John Wiley & Sons, Ltd, 2007) pp. 205–344.
- ⁷J. C. Grossman, M. Rohlfing, L. Mitas, S. G. Louie, and M. L. Cohen, “High accuracy many-body calculational approaches for excitations in molecules,” Phys. Rev. Lett. **86**, 472–475 (2001).
- ⁸C. Rostgaard, K. W. Jacobsen, and K. S. Thygesen, “Fully self-consistent gw calculations for molecules,” Phys. Rev. B **81**, 085103 (2010).
- ⁹X. Blase, C. Attaccalite, and V. Olevano, “First-principles GW calculations for fullerenes, porphyrins, phtalocyanine, and other molecules of interest for organic photovoltaic applications,” Phys. Rev. B **83**, 115103 (2011).
- ¹⁰F. Bruneval, “Ionization energy of atoms obtained from GW self-energy or from random phase approximation total energies,” J. Chem. Phys. **136**, 194107 (2012).
- ¹¹X. Ren, P. Rinke, V. Blum, J. Wieferink, A. Tkatchenko, A. Sanfilippo, K. Reuter, and M. Scheffler, “Resolution-of-identity approach to hartree–fock, hybrid density functionals, rpa, mp2 and gw with numeric atom-centered orbital basis functions,” New J. Phys. **14**, 053020 (2012).
- ¹²S. Sharifzadeh, I. Tamblyn, P. Doak, P. Darancet, and J. Neaton, “Quantitative molecular orbital energies within a g0w0 approximation,” Europ. Phys. J. B **85**, 323 (2012).
- ¹³T. Körzdörfer and N. Marom, “Strategy for finding a reliable starting point for G_0W_0 demonstrated for molecules,” Phys. Rev. B **86**, 041110 (2012).
- ¹⁴F. Bruneval and M. A. L. Marques, “Benchmarking the starting points of the gw approximation for molecules,” J. Chem. Theory Comput. **9**, 324–329 (2013), <http://pubs.acs.org/doi/pdf/10.1021/ct300835h>.
- ¹⁵P. Koval, D. Foerster, and D. Sánchez-Portal, “Fully self-consistent gw and quasiparticle self-consistent gw for molecules,” Phys. Rev. B **89**, 155417 (2014).
- ¹⁶M. J. van Setten, F. Caruso, S. Sharifzadeh, X. Ren, M. Scheffler, F. Liu, J. Lischner, L. Lin, J. R. Deslippe, S. G. Louie, C. Yang, F. Weigend, J. B. Neaton, F. Evers, and P. Rinke, “Gw100: Benchmarking g0w0 for molecular systems,” J. Chem. Theory Comput. **11**, 5665–5687 (2015), pMID: 26642984, <http://dx.doi.org/10.1021/acs.jctc.5b00453>.
- ¹⁷M. Govoni and G. Galli, “Large scale gw calculations,” J. Chem. Theory Comput. **11**, 2680–2696 (2015), pMID: 26575564, <http://dx.doi.org/10.1021/ct500958p>.
- ¹⁸J. W. Knight, X. Wang, L. Gallandi, O. Dolgounitcheva, X. Ren, J. V. Ortiz, P. Rinke, T. Körzdörfer, and N. Marom, “Accurate ionization potentials and electron affinities of acceptor molecules iii: A benchmark of gw methods,” Journal of Chemical Theory and Computation **12**, 615–626 (2016), <http://dx.doi.org/10.1021/acs.jctc.5b00871>.
- ¹⁹E. Maggio, P. Liu, M. J. van Setten, and G. Kresse, “Gw100: A plane wave perspective for small molecules,” Journal of Chemical Theory and Computation **13**, 635–648 (2017), <https://doi.org/10.1021/acs.jctc.6b01150>.

- ²⁰M. F. Lange and T. C. Berkelbach, "On the relation between equation-of-motion coupled-cluster theory and the gw approximation," *J. Chem. Theory Comput.* **14**, 4224–4236 (2018), <https://doi.org/10.1021/acs.jctc.8b00455>.
- ²¹G. Baym, "Self-consistent approximations in many-body systems," *Phys. Rev.* **127**, 1391–1401 (1962).
- ²²B. Holm, "Total energies from *GW* calculations," *Phys. Rev. Lett.* **83**, 788–791 (1999).
- ²³P. García-González and R. W. Godby, "Self-consistent calculation of total energies of the electron gas using many-body perturbation theory," *Phys. Rev. B* **63**, 075112 (2001).
- ²⁴F. Caruso, P. Rinke, X. Ren, M. Scheffler, and A. Rubio, "Unified description of ground and excited states of finite systems: The self-consistent *gw* approach," *Phys. Rev. B* **86**, 081102 (2012).
- ²⁵J. F. Dobson and J. Wang, "Successful test of a seamless van der waals density functional," *Phys. Rev. Lett.* **82**, 2123–2126 (1999).
- ²⁶F. Furche, "Molecular tests of the random phase approximation to the exchange-correlation energy functional," *Phys. Rev. B* **64**, 195120 (2001).
- ²⁷M. Fuchs, K. Burke, Y.-M. Niquet, and X. Gonze, "Comment on "total energy method from many-body formulation"," *Phys. Rev. Lett.* **90**, 189701 (2003).
- ²⁸J. Harl and G. Kresse, "Cohesive energy curves for noble gas solids calculated by adiabatic connection fluctuation-dissipation theory," *Phys. Rev. B* **77**, 045136 (2008).
- ²⁹S. Lebègue, J. Harl, T. Gould, J. G. Ángyán, G. Kresse, and J. F. Dobson, "Cohesive properties and asymptotics of the dispersion interaction in graphite by the random phase approximation," *Phys. Rev. Lett.* **105**, 196401 (2010).
- ³⁰L. Schimka, J. Harl, A. Stroppa, A. Grueneis, M. Marsman, F. Mittendorfer, and G. Kresse, "Accurate surface and adsorption energies from many-body perturbation theory," *Nat. Mater.* **9**, 741–744 (2010).
- ³¹X. Ren, P. Rinke, C. Joas, and M. Scheffler, "Random-phase approximation and its applications in computational chemistry and materials science," *J. Mater. Sci.* **47**, 21 (2012).
- ³²F. Bruneval, "Improved density matrices for accurate molecular ionization potentials," *Phys. Rev. B* **99**, 041118 (2019).
- ³³F. Bruneval, "Assessment of the linearized gw density matrix for molecules," *J. Chem. Theory Comput.* **15**, 4069–4078 (2019).
- ³⁴A. Klein, "Perturbation theory for an infinite medium of fermions. ii," *Phys. Rev.* **121**, 950–956 (1961).
- ³⁵J. M. Luttinger and J. C. Ward, "Ground-state energy of a many-fermion system. ii," *Phys. Rev.* **118**, 1417–1427 (1960).
- ³⁶V. M. Galitskii and A. B. Migdal, "Application of quantum field theory methods to the many body problem," *Sov. Phys. JETP* **139**, 96 (1958).
- ³⁷C.-O. Almbladh, U. V. Barth, and R. V. Leeuwen, "Variational total energies from Φ - and Ψ - derivable theories," *International Journal of Modern Physics B* **13**, 535–541 (1999), <http://www.worldscientific.com/doi/pdf/10.1142/S0217979299000436>.
- ³⁸N. E. Dahlen and U. von Barth, "Variational second-order möller-pletset theory based on the luttinger-ward functional," *The Journal of Chemical Physics* **120**, 6826–6831 (2004), <https://doi.org/10.1063/1.1650307>.
- ³⁹N. E. Dahlen and U. v. Barth, "Variational energy functionals tested on atoms," *Phys. Rev. B* **69**, 195102 (2004).
- ⁴⁰N. E. Dahlen, R. van Leeuwen, and U. von Barth, "Variational energy functionals of the green function and of the density tested on molecules," *Phys. Rev. A* **73**, 012511 (2006).
- ⁴¹A. Stan, N. E. Dahlen, and R. van Leeuwen, "Fully self-consistent *GW* calculations for atoms and molecules," *Europhys. Lett.* **76**, 298 (2006).
- ⁴²C. Holzer, X. Gui, M. E. Harding, G. Kresse, T. Helgaker, and W. Klopper, "Bethe–salpeter correlation energies of atoms and molecules," *J. Chem. Phys.* **149**, 144106 (2018), <https://doi.org/10.1063/1.5047030>.
- ⁴³P.-F. Loos, A. Scemama, I. Duchemin, D. Jacquemin, and X. Blase, "Pros and cons of the bethe–salpeter formalism for ground-state energies," *J. Phys. Chem. Lett.* **11**, 3536–3545 (2020), <https://doi.org/10.1021/acs.jpclett.0c00460>.
- ⁴⁴J. A. Berger, P.-F. Loos, and P. Romaniello, "Potential energy surfaces without unphysical discontinuities: the coulomb-hole plus screened exchange approach," (2020), arXiv:2008.12367 [physics.chem-ph].
- ⁴⁵A. Schindlmayr, "Violation of particle number conservation in the *GW* approximation," *Phys. Rev. B* **56**, 3528–3531 (1997).
- ⁴⁶A. Stan, N. E. Dahlen, and R. van Leeuwen, "Levels of self-consistency in the gw approximation," *J. Chem. Phys.* **130**, 114105 (2009), <http://dx.doi.org/10.1063/1.3089567>.
- ⁴⁷M. Hellgren, F. Caruso, D. R. Rohr, X. Ren, A. Rubio, M. Scheffler, and P. Rinke, "Static correlation and electron localization in molecular dimers from the self-consistent rpa and *gw* approximation," *Phys. Rev. B* **91**, 165110 (2015).
- ⁴⁸A. Kutepov, S. Y. Savrasov, and G. Kotliar, "Ground-state properties of simple elements from gw calculations," *Phys. Rev. B* **80**, 041103 (2009).
- ⁴⁹A. L. Kutepov, "Ground state properties of 3d metals from self-consistent *GW* approach," *Journal of Physics: Condensed Matter* **29**, 465503 (2017).
- ⁵⁰A. Kutepov, "Self-consistent gw method: $O(n)$ algorithm for polarizability and self energy," *Computer Physics Communications* **257**, 107502 (2020).
- ⁵¹G. D. Mahan, *Many-Particle Physics*, 3rd ed. (Kluwer Academic/Plenum Publishers, 2000).
- ⁵²Note that v_{xc} may represent any mean-field approximation, not only a Kohn-Sham potential but also any non-local generalized Kohn-Sham potential (a so-called hybrid functional for instance).
- ⁵³L. Reining, "The gw approximation: content, successes and limitations," *Wiley Interdisciplinary Reviews: Computational Molecular Science* **8**, e1344 (2018), <https://onlinelibrary.wiley.com/doi/pdf/10.1002/wcms.1344>.
- ⁵⁴G. Baym and L. P. Kadanoff, "Conservation laws and correlation functions," *Phys. Rev.* **124**, 287–299 (1961).
- ⁵⁵A. L. Fetter and J. D. Walecka, *Quantum theory of Many-Particle Systems* (MacGraw-Hill, New York, 1971).
- ⁵⁶X. Ren, P. Rinke, G. E. Scuseria, and M. Scheffler, "Renormalized second-order perturbation theory for the electron correlation energy: Concept, implementation, and benchmarks," *Phys. Rev. B* **88**, 035120 (2013).
- ⁵⁷P. Hohenberg and W. Kohn, "Inhomogeneous electron gas," *Phys. Rev.* **136**, B864–B871 (1964).
- ⁵⁸Y. M. Niquet, M. Fuchs, and X. Gonze, "Exchange-correlation potentials in the adiabatic connection fluctuation-dissipation framework," *Phys. Rev. A* **68**, 032507 (2003).
- ⁵⁹L. J. Sham and M. Schlüter, "Density-functional theory of the energy gap," *Phys. Rev. Lett.* **51**, 1888–1891 (1983).
- ⁶⁰Y. M. Niquet, M. Fuchs, and X. Gonze, "Asymptotic behavior of the exchange-correlation potentials from the linear-response sham–schlüter equation," *J. Chem. Phys.* **118**, 9504–9518 (2003), <https://doi.org/10.1063/1.1566739>.
- ⁶¹M. L. Tiago, S. Ismail-Beigi, and S. G. Louie, "Effect of semicore orbitals on the electronic band gaps of si, ge, and gaas within the *GW* approximation," *Phys. Rev. B* **69**, 125212 (2004).
- ⁶²M. J. van Setten, F. Weigend, and F. Evers, "The gw-method for quantum chemistry applications: Theory and implementation," *J. Chem. Theory Comput.* **9**, 232–246 (2013), pMID: 26589026, <http://dx.doi.org/10.1021/ct300648t>.
- ⁶³F. Bruneval, T. Rangel, S. M. Hamed, M. Shao, C. Yang, and J. B. Neaton, "molgw 1: Many-body perturbation theory software for atoms, molecules, and clusters," *Comput. Phys. Commun.* **208**, 149 – 161 (2016).
- ⁶⁴M. E. Casida, "Recent advances in density functional methods, Part I," (World Scientific, Singapore, 1995) p. 155.
- ⁶⁵M. Marques and E. Gross, "Time-dependent density functional theory," *Annu. Rev. Phys. Chem.* **55**, 427–455 (2004), pMID: 15117259, <http://dx.doi.org/10.1146/annurev.physchem.55.091602.094449>.
- ⁶⁶F. Caruso, *Self-consistent *GW* approach for the unified descrip-*

- tion of ground and excited states of finite systems*, Ph.D. thesis (2013).
- ⁶⁷V. Blum, R. Gehrke, F. Hanke, P. Havu, V. Havu, X. Ren, K. Reuter, and M. Scheffler, “Ab initio molecular simulations with numeric atom-centered orbitals,” *Comput. Phys. Commun.* **180**, 2175–2196 (2009).
- ⁶⁸S. Obara and A. Saika, “Efficient recursive computation of molecular integrals over cartesian gaussian functions,” *J. Chem. Phys.* **84**, 3963–3974 (1986).
- ⁶⁹E. F. Valeev, “A library for the evaluation of molecular integrals of many-body operators over gaussian functions,” (2016).
- ⁷⁰T. H. Dunning, “Gaussian basis sets for use in correlated molecular calculations. i. the atoms boron through neon and hydrogen,” *J. Chem. Phys.* **90**, 1007–1023 (1989).
- ⁷¹I. Y. Zhang, X. Ren, P. Rinke, V. Blum, and M. Scheffler, “Numeric atom-centered-orbital basis sets with valence-correlation consistency from h to ar,” *New J. Phys.* **15**, 123033 (2013).
- ⁷²K. Eichkorn, O. Treutler, H. Öhm, M. Häser, and R. Ahlrichs, “Auxiliary basis sets to approximate coulomb potentials,” *Chem. Phys. Lett.* **240**, 283–290 (1995).
- ⁷³F. Weigend, M. Häser, H. Patzelt, and R. Ahlrichs, “Ri-mp2: optimized auxiliary basis sets and demonstration of efficiency,” *Chem. Phys. Lett.* **294**, 143–152 (1998).
- ⁷⁴M. Rohlfling, “Excited states of molecules from green’s function perturbation techniques,” *Int. J. Quantum Chem.* **80**, 807 (2000).
- ⁷⁵R. Yang, A. P. Rendell, and M. J. Frisch, “Automatically generated coulomb fitting basis sets: Design and accuracy for systems containing h to kr,” *J. Chem. Phys.* **127**, 074102 (2007), <https://doi.org/10.1063/1.2752807>.
- ⁷⁶M. J. Frisch, G. W. Trucks, H. B. Schlegel, G. E. Scuseria, M. A. Robb, J. R. Cheeseman, G. Scalmani, V. Barone, G. A. Petersson, H. Nakatsuji, X. Li, M. Caricato, A. V. Marenich, J. Bloino, B. G. Janesko, R. Gomperts, B. Mennucci, H. P. Hratchian, J. V. Ortiz, A. F. Izmaylov, J. L. Sonnenberg, D. Williams-Young, F. Ding, F. Lipparini, F. Egidi, J. Goings, B. Peng, A. Petrone, T. Henderson, D. Ranasinghe, V. G. Zakrzewski, J. Gao, N. Rega, G. Zheng, W. Liang, M. Hada, M. Ehara, K. Toyota, R. Fukuda, J. Hasegawa, M. Ishida, T. Nakajima, Y. Honda, O. Kitao, H. Nakai, T. Vreven, K. Throssell, J. A. Montgomery, Jr., J. E. Peralta, F. Ogliaro, M. J. Bearpark, J. J. Heyd, E. N. Brothers, K. N. Kudin, V. N. Staroverov, T. A. Keith, R. Kobayashi, J. Normand, K. Raghavachari, A. P. Rendell, J. C. Burant, S. S. Iyengar, J. Tomasi, M. Cossi, J. M. Millam, M. Klene, C. Adamo, R. Cammi, J. W. Ochterski, R. L. Martin, K. Morokuma, O. Farkas, J. B. Foresman, and D. J. Fox, “Gaussian[™]16 Revision B.01,” (2016), gaussian Inc. Wallingford CT.
- ⁷⁷X. Blase, P. Boulanger, F. Bruneval, M. Fernandez-Serra, and I. Duchemin, “*gw* and bethe-salpeter study of small water clusters,” *J. Chem. Phys.* **144**, 034109 (2016).
- ⁷⁸F. Caruso, P. Rinke, X. Ren, A. Rubio, and M. Scheffler, “Self-consistent *gw*: All-electron implementation with localized basis functions,” *Phys. Rev. B* **88**, 075105 (2013).
- ⁷⁹M. Ernzerhof and G. E. Scuseria, “Assessment of the perdew–burke–ernzerhof exchange–correlation functional,” *J. Chem. Phys.* **110**, 5029–5036 (1999), <https://doi.org/10.1063/1.478401>.
- ⁸⁰J. P. Perdew, K. Burke, and M. Ernzerhof, “Generalized gradient approximation made simple,” *Phys. Rev. Lett.* **77**, 3865–3868 (1996).
- ⁸¹C. Adamo and V. Barone, “Toward reliable density functional methods without adjustable parameters: The pbe0 model,” *J. Chem. Phys.* **110**, 6158–6170 (1999).
- ⁸²M. Rodriguez-Mayorga, E. Ramos-Cordoba, P. Salvador, M. Solà, and E. Matito, “Bonding description of the harpoon mechanism,” *Mol. Phys.* **114**, 1345 (2016).
- ⁸³M. Fuchs and X. Gonze, “Accurate density functionals: Approaches using the adiabatic-connection fluctuation-dissipation theorem,” *Phys. Rev. B* **65**, 235109 (2002).
- ⁸⁴M. Fuchs, Y.-M. Niquet, X. Gonze, and K. Burke, “Describing static correlation in bond dissociation by kohn–sham density functional theory,” *J. Chem. Phys.* **122**, 094116 (2005), <https://doi.org/10.1063/1.1858371>.
- ⁸⁵H.-V. Nguyen and G. Galli, “A first-principles study of weakly bound molecules using exact exchange and the random phase approximation,” *J. Chem. Phys.* **132**, 044109 (2010), <https://doi.org/10.1063/1.3299247>.